Electronic Supplementary Material (ESI) for Inorganic Chemistry Frontiers.

Supporting Information

Achieving photocatalytic hydrogen production from alkaline solution upon designed mesoporous TiO_2-Ni hybrid employing commonly-used paper as sacrificial electron donor

Yi Wei [a], Jinyan Xiong [b], Weijie Li [c], Ravichandran H Kollarigowda [d], Gang Cheng [a*]

[a] School of Chemistry and Environmental Engineering, Wuhan Institute of Technology, Xiongchu Avenue, Wuhan 430073, PR China

[b] College of Chemistry and Chemical Engineering, Wuhan Textile University, Wuhan 430200, China

[c] Institute for Superconducting and Electronic Materials, University of Wollongong, Innovation Campus, Squires Way, North Wollongong, NSW 2500, Australia

[d] Department of Materials Science Engineering, University of Illinois at Urbana–Champaign, 1304 W Green St, Urbana, IL 61801.

[*]Corresponding author:

gchenglab@163.com (G. Cheng); Telefax: +862787195680

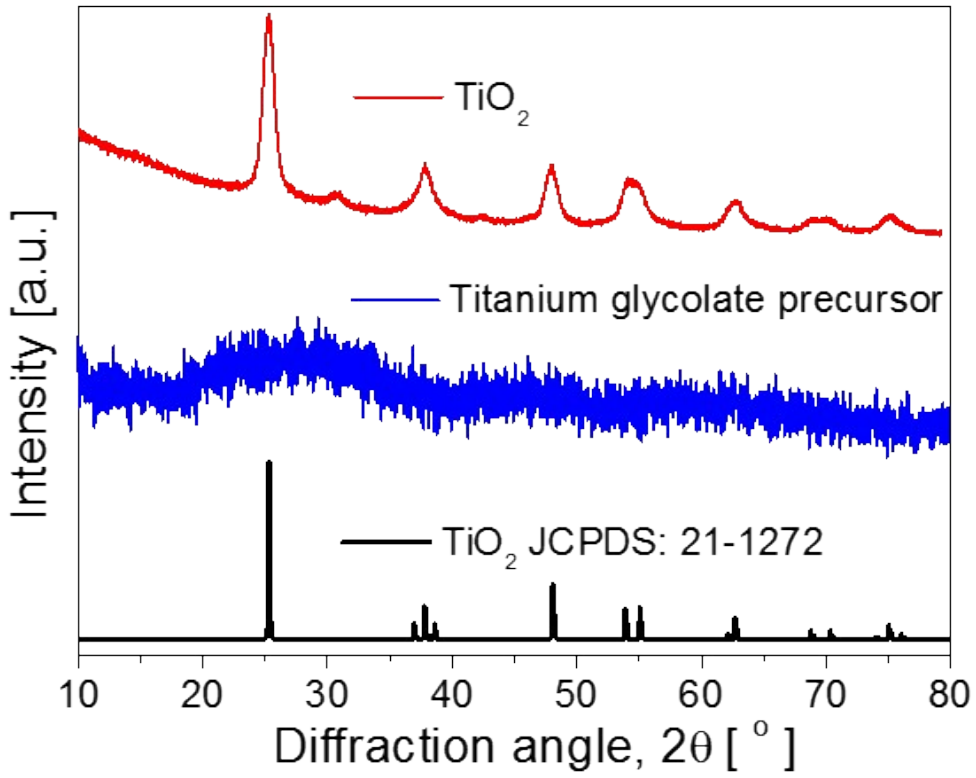

Figure S1. XRD patterns of as-prepared titanium glycolate precursor and TiO_2.

The XRD patterns of titanium glycolate precursor in Figure S1 shows non-crystal structure. After treated by hydrothermal reaction, the well-crystallized TiO_2, indexed to tetragonal TiO_2 (JCPDS Card No. 21-1272), was obtained.

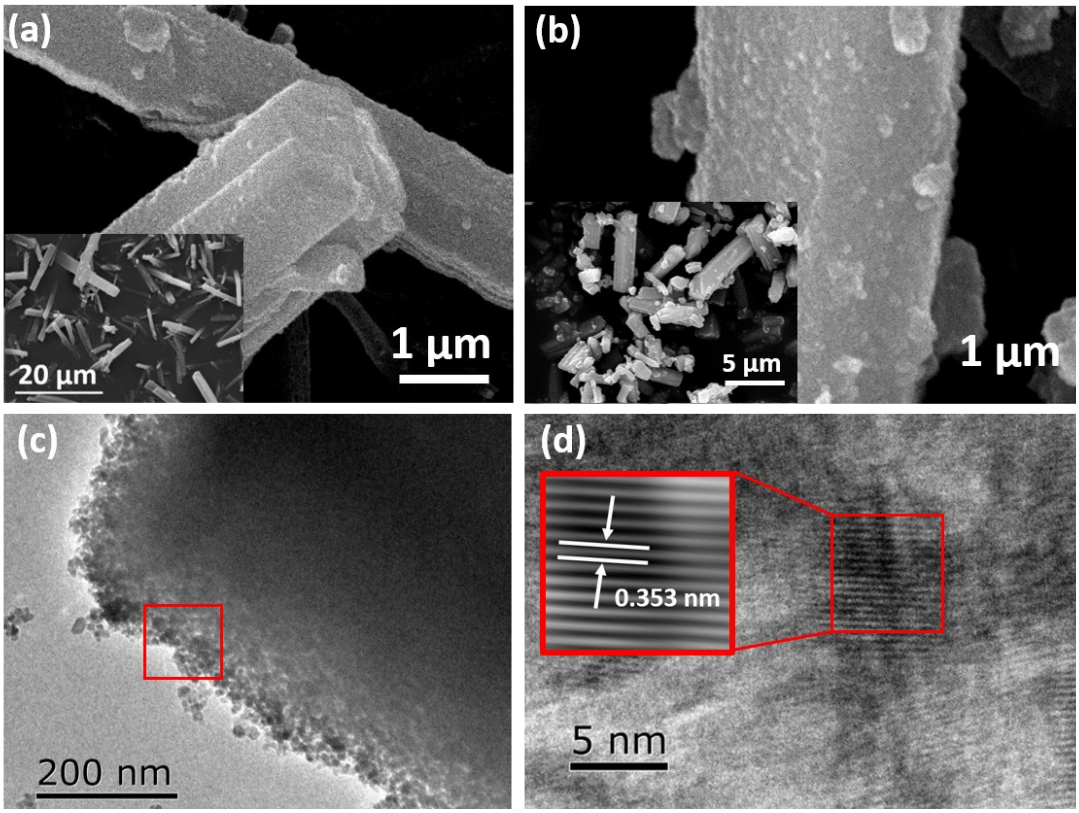

Figure S2. (a) SEM images of titanium glycolate precursor, (b) SEM image, (c) TEM image and (d) HRTEM image of as-prepared TiO_2.

The titanium glycolate precursor from the SEM image shows a microrod-like morphology in Figure S2a. After being treated with hydrothermal reaction, the SEM image of the formed TiO_2 in Figure S2b also shows microrod-like structure, indicating that the hydrothermal reaction did not change their morphology from titanium glycolate precursor to TiO_2. To further investigate the morphology of TiO_2, TEM characterization was employed. As shown in figure S2c, the microrod-like TiO_2 comprise small nanoparticles forming a mesoporous structure. The corresponding TRTEM image is shown in Figure S2d, it is observed that the TiO_2 nanoparticles show clear lattice fringes with a d-spacing of 0.353 nm, which can be assigned to (101) planes of TiO_2.

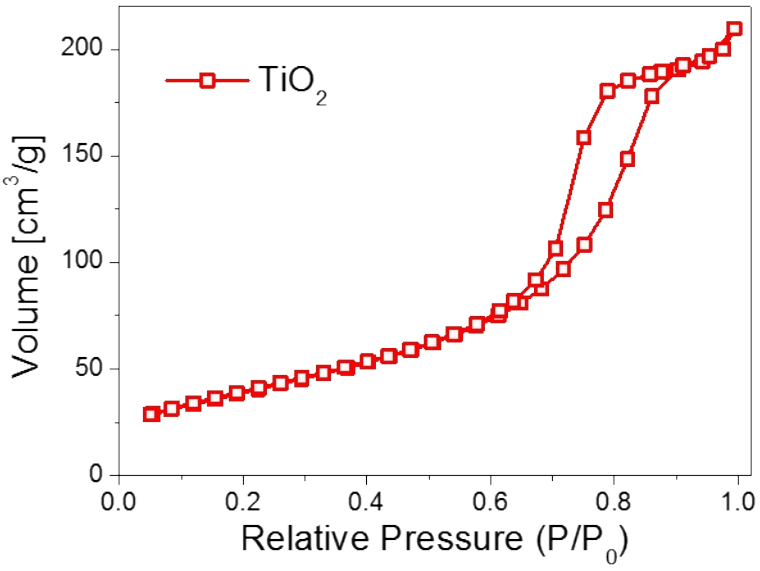

Figure S3. N_2 adsorption-desorption isotherms of as-prepared TiO_2.

Figure S3 shows the nitrogen adsorption-desorption isotherms of TiO_2, which display typical type IV pattern in the range 0.5-1.0 P/P_0, indicating the characteristic of mesoporous materials. The BET surface area of the TiO_2 was calculated to be 159.6 m^2/g. The large surface area would accelerate the photocatalytic performance.

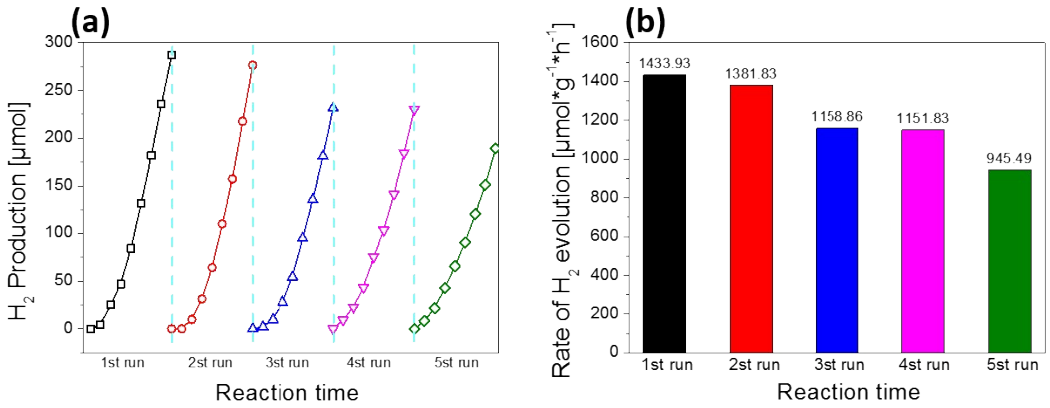

Figure S4. (a) Photocatalytic hydrogen evolution performance and (b) hydrogen evolution rate during five consecutive runs over TiO_2-Ni-1% hybrid.

The TiO_2-Ni-1% hybrid showed good hydrogen evolution performance with the rate of 945.49 μmol g^{-1} h^{-1} after five cycling test. It was obvious that the sample showed a slightly decreased hydrogen evolution rate, which indicated that the hybrid can be stable for certain period of time in photocatalytic hydrogen evolution while the long-term stability of the present TiO_2-Ni-1% hybrid still need to be improved for future study.

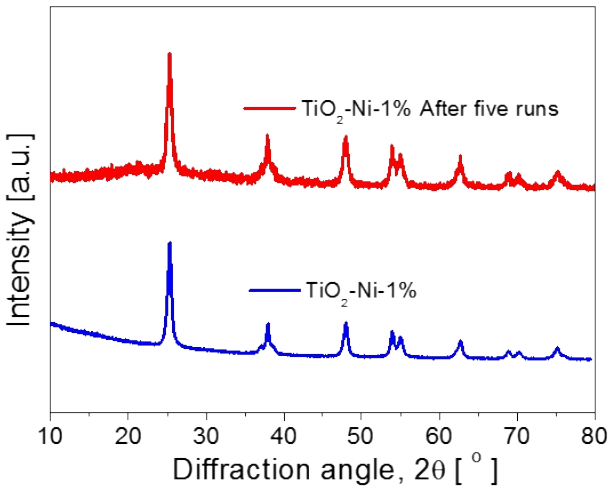

Figure S5. XRD patterns of the as-prepared TiO_2-Ni-1% before and after cycling hydrogen evolution experiments.

The XRD patterns of as-prepared TiO_2-Ni-1% before and after cycling hydrogen evolution experiments are shown in figure S5. It could be observed that the two samples showed the same diffraction peaks, which indicated that the as-prepared TiO_2-Ni-1% photocatalyst had good stability under artificial solar light irradiation.

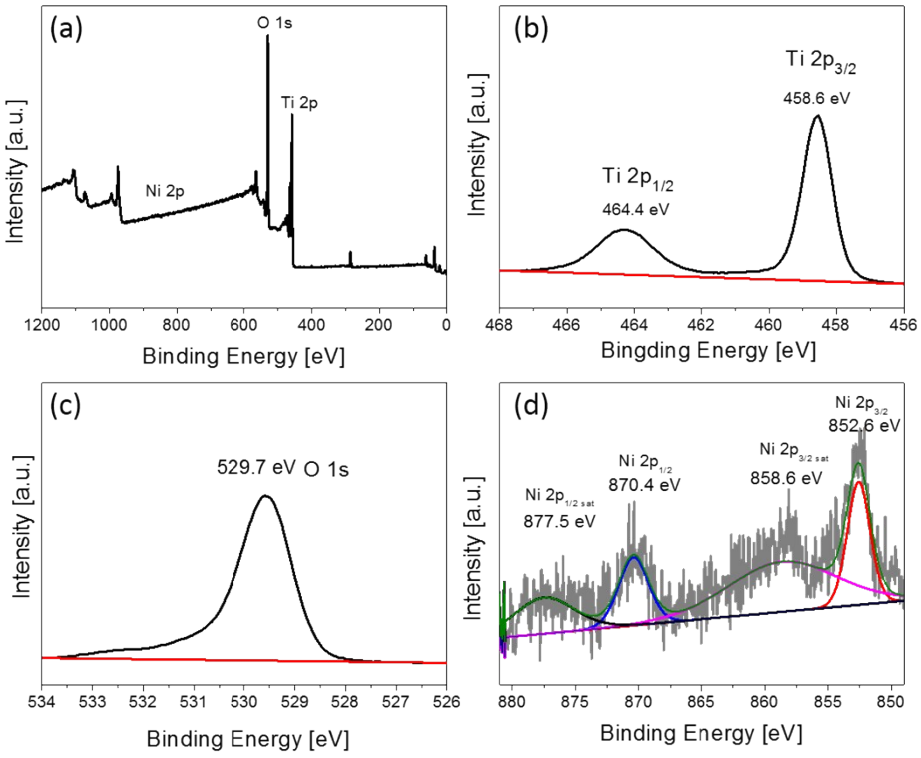

Figure S6. (a) XPS survey spectra, (b) Ti 2p binding energy, (c) O 1s binding energy, (d) Ni 2p binding energy peaks of TiO_2-Ni-1% (after five consecutive runs).

The chemical state of each element was investigated by XPS measurement. It was observed that the chemical state of Ti, O, and Ni elements are similar with that of previous hybrid, indicating the good chemical stability of TiO_2-Ni-1% for photocatalytic hydrogen evolution.

Table S1. The Ni content parameters of ICP-AES of different photocatalysts.

Sample	wt%
TiO_2	0
TiO_2-Ni-0.5%	0.41%
TiO_2-Ni-1%	0.94%
TiO_2-Ni-2%	2.25%
TiO_2-Ni-3%	3.66%

Table S2. Photocatalytic activities towards hydrogen evolution on different photocatalysts.

Photocatalyst	Substrate	Light source	Rate (μmol/g/h)	Reference
$Pt/Zn(OH)_2/Cd_{0.3}Zn_{0.7}S$	Na_2S/Na_2SO_3	450 nm	7470	[1]
$Pt/Cu_{1.94}S\text{-}Zn_xCd_{1-x}S$	Na_2S/Na_2SO_3	420 nm	13533	[2]
$Cd_{0.4}Zn_{0.6}S/TiO_2$	Na_2S/Na_2SO_3	450 nm	1800	[3]
$Pt/Cd_{0.6}Zn_{0.4}S$	Na_2S/Na_2SO_3	450 nm	3400	[4]
Ni/TiO_2	methanol	Artificial solar light	1433	Present study
Ni/TiO_2	Paper	Artificial solar light	253	Present study

Reference

[1] D.V. Markovskaya, E.A. Kozlova, S.V. Cherepanova, A.A. Saraev, E.Y. Gerasimov, V.N. Parmon, Synthesis of $Pt/Zn(OH)_2/Cd_{0.3}Zn_{0.7}S$ for the photocatalytic hydrogen evolution from aqueous solutions of organic and inorganic electron donors under visible light. *Topics in Catalysis* **2016**, 59, 1297-1304.

[2] Y. Chen, S. Zhao, X. Wang, Q. Peng, R. Lin, Y. Wang, R. Shen, X. Cao, L. Zhang, G. Zhou, J. Li, A. Xia, Y. Li, Synergetic integration of $Cu_{1.94}S–Zn_xCd_{1–x}S$ heteronanorods for enhanced visible-light-driven photocatalytic hydrogen production. *Journal of the American Chemical Society* **2016**, 138, 4286-4289.

[3] E.A. Kozlova, A.Y. Kurenkova, V.S. Semeykina, E.V. Parkhomchuk, S.V. Cherepanova, E.Y. Gerasimov, A.A. Saraev, V.V. Kaichev, V.N. Parmon, Effect of titania regular macroporosity on the photocatalytic hydrogen evolution on $Cd_{1–x}Zn_xS/TiO_2$ catalysts under visible light. *ChemCatChem* **2015**, 7, 4108-4117.

[4] E.A. Kozlova, S.V. Cherepanova, D.V. Markovskaya, A.A. Saraev, E.Y. Gerasimov, V.N. Parmon, Novel photocatalysts $Pt/Cd_{1–x}Zn_xS/ZnO/Zn(OH)_2$: Activation during hydrogen evolution from aqueous solutions of ethanol under visible light. *Applied Catalysis B: Environmental* **2016**, 183, 197-205.